LM-04K041
June 9, 2004

Hybrid Back Surface Reflector GaInAsSb Thermophotovoltaic Devices

R.K. Huang, C.A. Wang, M.K. Connors, G.W. Turner and M. Dashiell

Hybrid Back Surface Reflector GaInAsSb Thermophotovoltaic Devices

Robin K. Huang, Christine A. Wang, Michael K. Connors, George W. Turner
Lincoln Laboratory, Massachusetts Institute of Technology, 244 Wood St, Lexington, MA 02420-9108

Michael Dashiell
Lockheed Corporation, Schenectady, NY 12301

Abstract Back surface reflectors have the potential to improve thermophotovoltaic (TPV) device performance though the recirculation of infrared photons. The "hybrid" back-surface reflector (BSR) TPV cell approach allows one to construct BSRs for TPV devices using conventional, high efficiency, GaInAsSb-based TPV material. The design, fabrication, and measurements of hybrid BSR-TPV cells are described. The BSR was shown to provide a 4 mV improvement in open-circuit voltage under a constant short-circuit current, which is comparable to the 5 mV improvement theoretically predicted. Larger improvements in open-circuit voltage are expected in the future with materials improvements.

Introduction

System efficiency is a key driver for the development of TPV technology and cells [1]. While quantum efficiency and fill factor are approaching their practical limiting values in state-of-the-art 0.54 eV GaInAsSb/GaSb TPV cells, the voltage factor qV_{oc}/E_g is approximately 0.6, where q is the electronic charge, V_{oc} is the open-circuit voltage, and E_g is the material bandgap. The voltage factor is about 85% of the practical limit [2], and improvements in diode efficiency will primarily result from improvements in open-circuit voltage. Incorporation of a back-surface reflector (BSR) is one potential approach to improve the V_{oc} of TPV cells. One technique to implement a BSR using 0.54-eV GaInAsSb/GaSb TPV material is the "hybrid" BSR-TPV approach [3], [4]. In the GaSb material system, semi-insulating substrates are not available. Therefore, to reduce losses due to free-carrier absorption, an n-type GaSb substrate is thinned and polished to a thickness of 100 μm to allow for high optical transmission in the 2.1 μm to 2.5 μm wavelength range. The "hybrid" BSR-TPV approach allows one to construct a dual-purpose n-type ohmic contact and back surface reflector. A similar approach is reported in reference [5], but no device performance improvements are demonstrated.

There are several potential advantages of the hybrid BSR-TPV. The open-circuit voltage V_{oc} can be increased due to (1) double pass of above bandgap photons to increase photon lifetime, and (2) increase of quantum efficiency, leading to an increase in V_{oc} though the short circuit current density J_{sc}, since $V_{oc} \approx (nkT/q)\ln(J_{sc}/J_s)$, where k is Boltzmann's constant, T is the device temperature, n is the ideality factor of the TPV

This work was sponsored by the Department of Energy under Air Force Contract No. F19628-00-C-0002. The opinions, interpretations, conclusions, and recommendations are those of the authors and are not necessarily endorsed by the United States Government.

diode, and J_s is the saturation current density. BSRs are used in TPV devices for double-pass of above bandgap photons and as a spectral control element [6], [7], [8]. These previous approaches have utilized monolithic integrated module (MIM) type devices with semi-insulating InP substrates [6], [7] or substrate-removed GaInAsSb-based devices [8].

"Buried" mirrors, requiring epitaxial lateral overgrowth or wafer fusion techniques, have also been proposed for GaSb-based TPV cells [9]. The "hybrid" BSR-TPV approach offers a viable method to achieve the advantages of the BSR for more conventional TPV structures in GaInAsSb-based TPV cells. Some practical advantages of the BSR-TPV include (1) conventional TPV material is utilized with no new epitaxy needed, (2) direct comparison is provided between reference and BSR cells using the same epitaxial growth, and (3) thinner substrates lead to improved heat removal.

Using PC1D device modeling software [10], we have calculated the expected dependence of V_{oc} in 0.54-eV GaInAsSb/GaSb TPV devices on surface recombination velocity (S) and bulk lifetime (τ_B). According to this model, the effect of a BSR on TPV performance was considered for two interesting cases. In case (1), assuming S = 1000 cm/s and τ_B = 1 μs, V_{oc} was calculated to be 317 mV for the BSR-TPV versus 312 mV for a conventional TPV device. Case (1) predicts a 5 mV improvement for the BSR-TPV device compared to the conventional TPV device. In case (2), assuming S = 10 cm/s and τ_B = 1 μs, V_{oc} was calculated to be 357 mV for the BSR-TPV versus 335 mV for a conventional TPV device. Case (2) predicts a 22 mV improvement when a BSR is incorporated in the TPV device. Case (1) represents the improvement in V_{oc} expected for current material [11], while case (2) represents the improvement expected for future material with reduced S values. Therefore, if we use current TPV material for BSR experiments, we should only expect to observe a modest 5 mV increase in V_{oc}.

Fabrication

A cross-sectional structure of the BSR-TPV cell is shown in figure 1. The device layers are epitaxially grown by OMVPE, and consist of (from top to bottom) a p-GaSb contact layer, a p-AlGaAsSb window layer to suppress surface recombination [12], a p-GaInAsSb layer, and an n-GaInAsSb layer, grown on an n-GaSb substrate. The total thickness of the device layers is about 5 to 6 μm. The n-GaSb substrate has been thinned and polished to about 100 μm in order to minimize free-carrier absorption for the BSR double-pass absorption. The front side metallization is in a typical TPV grid configuration. The backside dielectric and metallization is a hybrid BSR and ohmic contact design.

Experiments were performed to check the reflectivity of the n-GaSb in the presence of free carrier absorption in the doped material. An n-type GaSb substrate, doped in the low 10^{17} cm^{-3} range, was thinned and polished to a thickness of 100 μm. A hybrid BSR/ohmic contact was deposited on the backside of the wafer. No coatings were deposited on the frontside of the sample. The measured optical reflectivity spectrum is shown in Figure 2. By illuminating this sample at normal incidence on the frontside, the measured reflectivity is about 90% in the 2.1micron to 2.5 micron wavelengthrange and

this level of reflectivity is expected to be sufficient to promote the effects of photon recycling in device performance.

Masks for both the frontside and backside processing of reference and BSR TPV cells were designed. The frontside mask pattern consisted of a two-level mask, involving a mesa-etch mask and an ohmic-contact mask. Designed for processing one quarter of a 2-inch wafer, six 0.5 cm by 1 cm cells and two 0.25 by 0.5 cm cells can be accommodated in one fabrication chip. The size of the two smaller cells was chosen from previous investigations of the size dependence on TPV performance. Mesa etching was selected instead of cleaving or saw cutting, as a means of electrical isolation of cells in the design to minimize sidewall damage [11], [13]. For TPV cell separation, the mask is designed to accommodate either cleaving or saw cutting.

The hybrid backside ohmic contact and BSR is constructed with a backside fabrication process. The open areas between the contacts are for the BSR, which consists of sputtered Al_2O_3/Ti/Au. The coverage of the BSR on the backside is approximately 90% by area. The mask is designed for a liftoff of the BSR, and subsequent evaporation of the n-type ohmic contact between the mirror segments.

The specific contact resisitivity of the n-GaSb ohmic contacts, consisting of Au/Sn/Ti/Pt/Au, has been measured by the Cox-Strack technique to be approximately 2.3×10^{-6} Ω-cm^2. The resulting contribution from the hybrid BSR/contact to the diode series resistance is expected to be negligible compared with the typical 1-2 mΩ series resistance of these diodes.

After fabrication of both reference and BSR cells, the devices are packaged onto copper submounts with indium solder for improved thermal management and to facilitate testing (particularly for the 100-μm-thick BSR cells, which are fragile). A metallized ceramic flat is used as a contact pad for the device busbar, and multiple wirebond connections are made from the contact pad to the busbar to ensure electrical current uniformity.

Device Measurements

Illuminated I-V measurements are performed with the packaged device bolted to a copper heatsink on top of a thermoelectric cooler. In figure 3, illuminated I-V characteristics of a BSR cell (size approximately 0.7 cm by 0.5 cm) at a heatsink temperature of T=10° C, fabricated from wafer 01-499 are shown. Excellent TPV diode performance is apparent from these multiple intensity characteristics. The extracted J_{sc} versus V_{oc} is shown in figure 4 for the BSR and reference TPV cells at T=10° C, and in figure 5 for the BSR and reference TPV cells at T=25° C. At a fixed J_{sc}=2.2 A/cm^2, at T=10° C, V_{oc}=341 mV for the BSR cell as compared with V_{oc}=336 mV for the reference cell. At this same current density at T=25° C, V_{oc}=317 mV for the BSR cell as compared with V_{oc}=312 mV for the reference cell. The improvement in V_{oc} is about 4 to 5 mV at both temperatures, as expected from the calculations discussed earlier. Moreover, the fill factor of the BSR cells was better than that of the reference cell at both temperatures. At

T=25° C, the fill factor of the BSR cell was 66%, as compared with 65% for the reference cell. At T=10° C, the fill factor of the BSR cell was 71%, as compared with 67% for the reference cell. The difference in the slopes of the fitted lines in figure 5 is not well understood at this time. Similar experiments performed on BSR and reference TPV cells of the same size (1 cm by 0.5 cm) indicated similar improvements in V_{oc}, approximately 3 mV at both 10° and 25° C.

External quantum efficiency measurements were also performed on BSR and reference TPV cells. For this experiment, a BSR and a reference cell, both of which were nominally the same size (1 cm by 0.5 cm) were used so that neither illumination nor current nonuniformities in the measurement should lead to any experimental artifacts. Since these devices do not have anti-reflection coated, their peak external quantum efficiency is limited to about 67%. Similarly to our previous measurements [11], an improvement in external quantum efficiency could be observed near the bandedge of GaInAsSb (see figure 6). The fractional improvement of EQE is about 25% at a wavelength of 2.4 μm.

Conclusion

In summary, BSR-TPV cells have been demonstrated with a 4 mV improvement in V_{oc} (potentially limited by surface recombination) and improved external quantum efficiency at room temperature. This improvement is consistent with that predicted from theoretical calculations. Further improvements in V_{oc} are expected with improvements in material and interface quality. According to our calculations, if S can be decreased to about 10 cm/s [14], BSR-TPV cells will enable voltage factors as high as 0.66, which is 10% higher than that of the highest voltage factors obtained with state-of-the art 0.54-eV TPV cells.

Acknowledgements

The authors acknowledge L. J. Missaggia for packaging of TPV cells. This work was sponsored by the Department of Energy under Air Force Contract No. F19628-00-C-0002. The opinions, interpretations, conclusions, and recommendations are those of the authors and are not necessarily endorsed by the United States Government.

References

[1] T. J. Coutts, "Thermophotovoltaic generation of electricity," in *Clean energy from photovoltaics*, M.D. Archer and R. Hill, Ed. London: Imperial College Press, 2001, pp. 481-528.

[2] P. F. Baldasaro, E. J. Brown, D. M. Depoy, B. C. Campbell, and J. R. Parrington, "Experimental assessment of low temperature voltaic energy conversion," AIP Conf. Proc. 321, p. 29-43 (1994).

[3] G. W. Charache, D. M. DePoy, P. F. Baldasaro, and B. C. Campbell, "Thermophotovoltaic devices utilizing a back surface reflector for spectral control," AIP Conf. Proc. 358, p. 339 (1995).

[4] G. W. Charache, et al, "InGaAsSb thermophotovoltaic diode: physics evaluation," J. Appl. Phys., 85, 2247-52 (1999).

[5] Z. A. Shellenbarger, et al, "Improvements in GaSb-based thermophotvoltaic cells," AIP Conf. Proc. 401, p. 117-28 (1997).

[6] T. J. Coutts and J. S. Ward, "Thermophotovoltaic and photovoltaic conversion at high-flux densities," IEEE Trans. Electron. Devices, 46, p. 2145-53 (1999).

[7] R. R. Siergiej, et al, "20% efficient InGaAs/InPAs thermophotovoltaic cells," AIP Conf. Proc. 653, p. 414-23 (2003).

[8] C. A. Wang, et al, "Monolithically series-interconnected GaInAsSb/AlGaAsSb/ GaSb thermophotovoltaic devices with an internal back surface reflector formed by wafer bonding," Appl. Phys. Lett. 83, 1286 (2003).

[9] M. G. Mauk, et al, "New concepts for III-V antimonide thermophotovoltaics," AIP Conf. Proc. 401, p. 129-37 (1997).

[10] D. A. Clugston and P. A. Basore, "PC1D version 5: 32-bit solar cell modeling on personal computers," Conf. Rec. 26th IEEE Photovoltaics Specialists Conf., p. 207-10 (1997).

[11] C. A. Wang, et al, "Lattice-matched GaInAsSb/AlGaAsSb/GaSb Materials for Thermophotovoltaic Devices,"AIP Conf. Proc. 653, p. 324-34 (2003).

[12] H. K. Choi, et al, "High-performance GaInAsSb thermophotovoltaic devices with an AlGaAsSb window," Appl. Phys. Lett. 71, 3758 (1997).

[13] Z. A. Shellenbarger, et al, "High performance InGaAsSb TPV cells via multi-wafer OMVPE growth,"AIP Conf. Proc. 653, p. 314-23 (2003).

[14] C. A. Wang, et al, "Effect of growth interruption on surface recombination velocity in GaInAsSb/AlGaAsSb heterostructures grown by organometallic vapor phase epitaxy," Conf. Proc. 12th International Conference on Metal Organic Vapor Phase Epitaxy (2004).

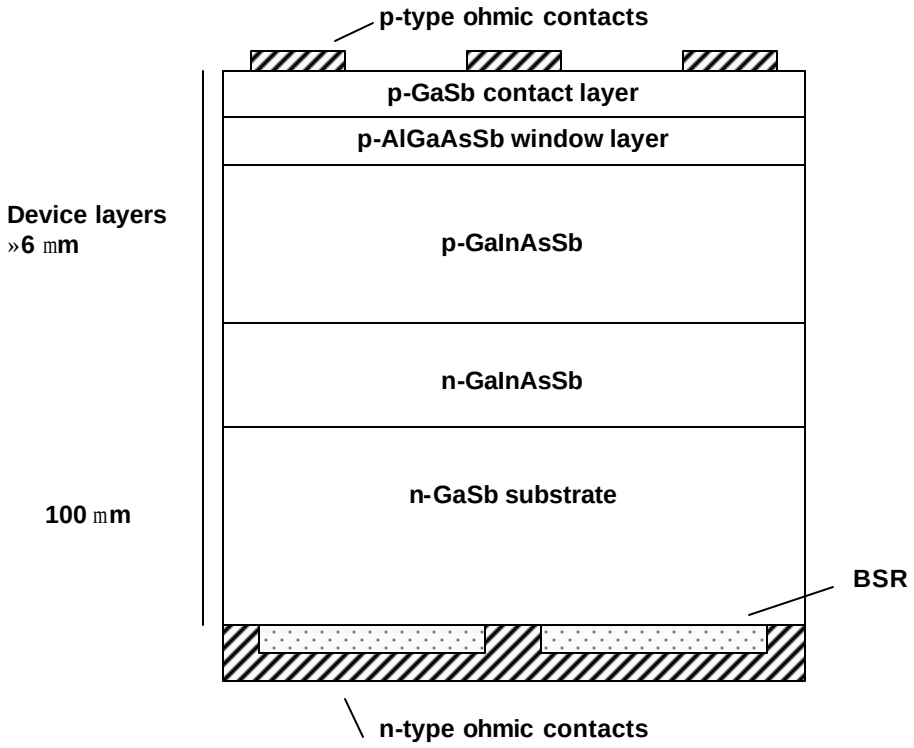

Figure 1. Cross-section of BSR-TPV cell. This drawing is not to scale.

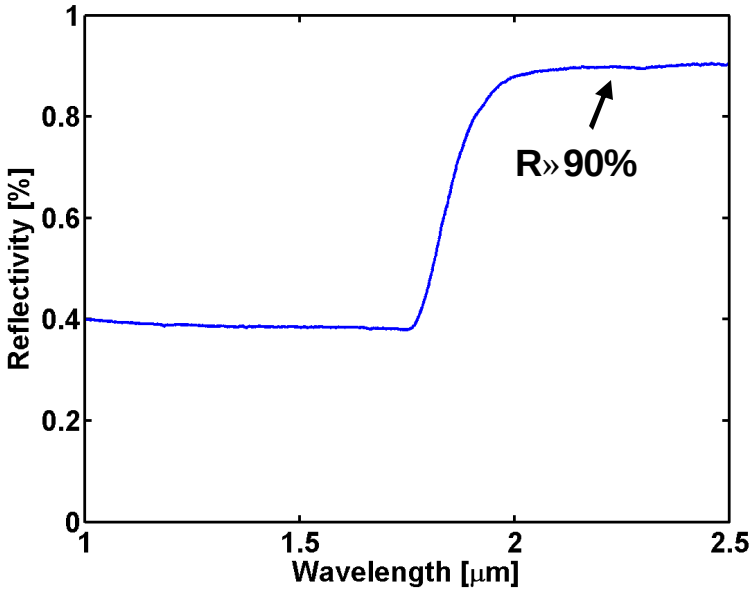

Figure 2. Reflectivity of BSR through 100 μm thick n-GaSb substrate.

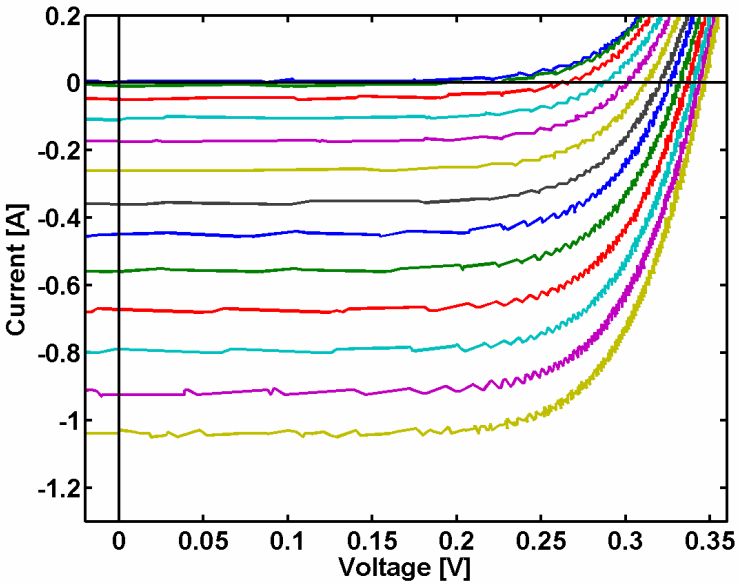

Figure 3. Multiple light intensity measurements on 01-499 BSR cell at a heatsink temperature of T=10° C.

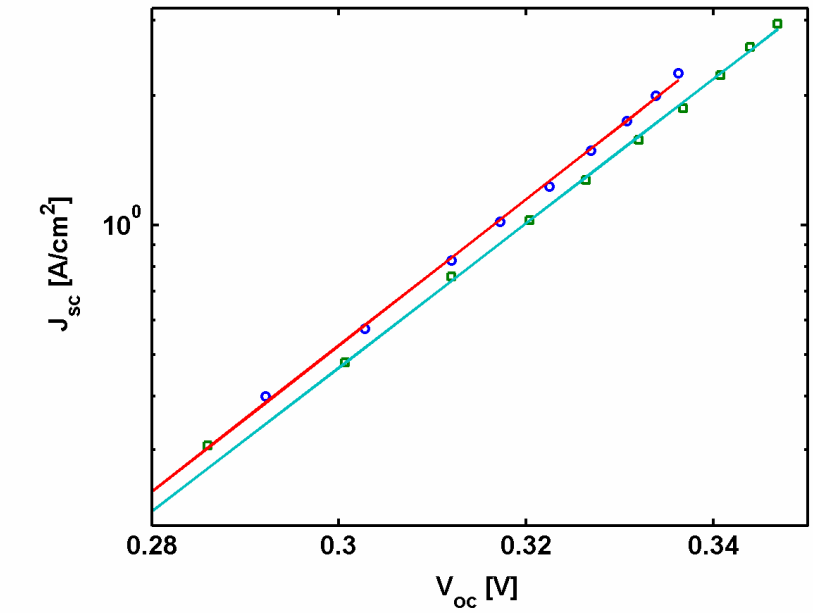

Figure 4. J_{sc} versus V_{oc} for 01-499 BSR cell (squares) and 01-499 reference cell (circles) at T=10° C.

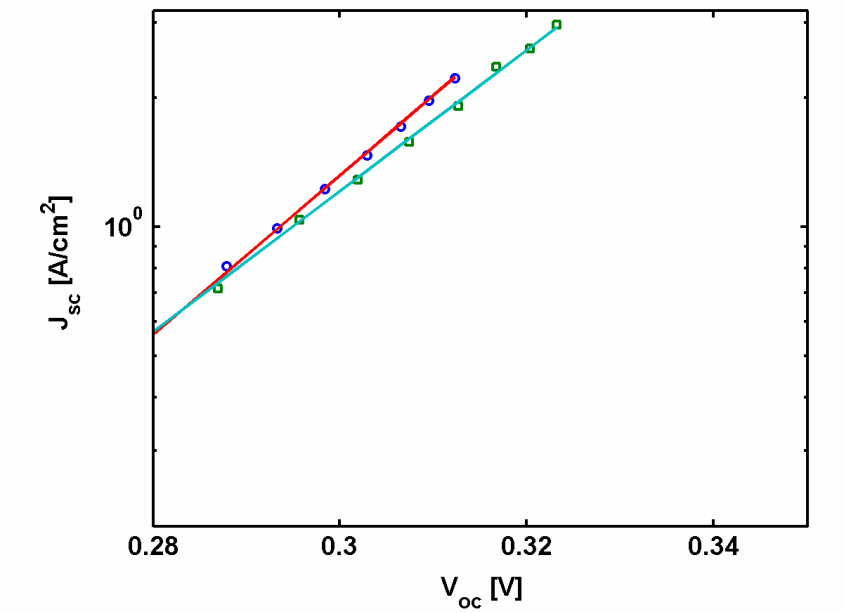

Figure 5. J_{sc} versus V_{oc} for 01-499 BSR cell (squares) and 01-499 reference cell (circles) at T=25° C.

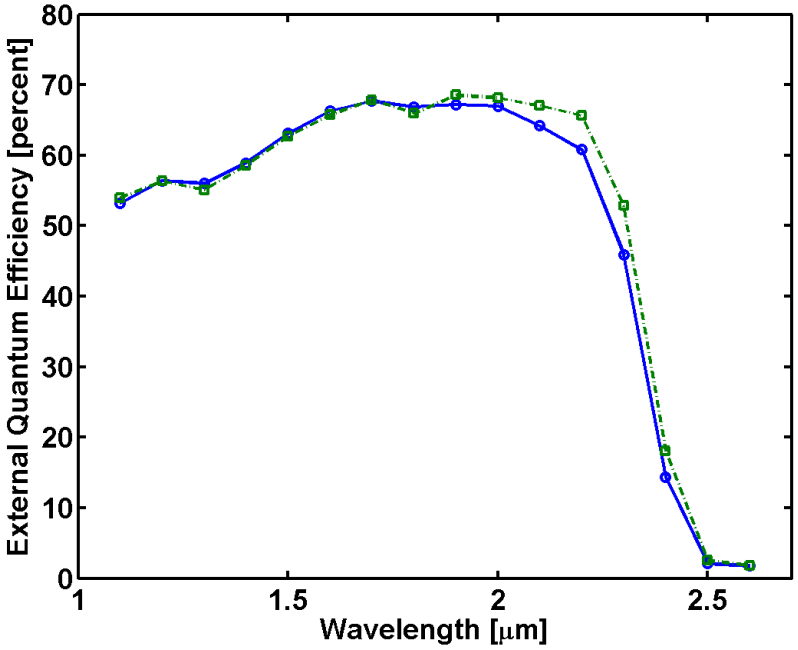

Figure 6. External quantum efficiency for 01-499 BSR cell (squares) and 01-499 reference cell (circles) at room temperature. Both devices are uncoated.